SCIENTIFIC REPORTS

OPEN

SUBJECT AREAS:

SUPERCONDUCTING PROPERTIES AND MATERIALS

SURFACES, INTERFACES AND THIN FILMS

ELECTRONIC PROPERTIES AND MATERIALS

Received
16 April 2014

Accepted
25 July 2014

Published
12 August 2014

Correspondence and requests for materials should be addressed to J.W. (jianwangphysics@pku.edu.cn) or L.W. (liliwang@mail.tsinghua.edu.cn)

* These authors contributed equally to this work.

High temperature superconducting FeSe films on $SrTiO_3$ substrates

Yi Sun[1]*, Wenhao Zhang[2,3]*, Ying Xing[1], Fangsen Li[2,3], Yanfei Zhao[1], Zhengcai Xia[5], Lili Wang[2,3,4], Xucun Ma[2,3,4], Qi-Kun Xue[2,4] & Jian Wang[1,4]

[1]International Center for Quantum Materials, School of Physics, Peking University, Beijing 100871, China, [2]State Key Laboratory of Low-Dimensional Quantum Physics, Department of Physics, Tsinghua University, Beijing 100084, China, [3]Institute of Physics, Chinese Academy of Sciences, Beijing 100190, China, [4]Collaborative Innovation Center of Quantum Matter, Beijing 100871, China, [5]Wuhan National High Magnetic Field Center, Huazhong University of Science and Technology, 1037 Luoyu road, Wuhan 430071, China.

Interface enhanced superconductivity at two dimensional limit has become one of most intriguing research directions in condensed matter physics. Here, we report the superconducting properties of ultra-thin FeSe films with the thickness of one unit cell (1-UC) grown on conductive and insulating $SrTiO_3$ (STO) substrates. For the 1-UC FeSe on conductive STO substrate (Nb-STO), the magnetization *versus* temperature (*M-T*) measurement shows a drop crossover around 85 K. For the FeSe films on insulating STO substrate, systematic transport measurements were carried out and the sheet resistance of FeSe films exhibits Arrhenius TAFF behavior with a crossover from a single-vortex pinning region to a collective creep region. More intriguing, sign reversal of Hall resistance with temperature is observed, demonstrating a crossover from hole conduction to electron conduction above T_C in 1-UC FeSe films.

Iron-based superconductors has triggered great interest[1] because of the high transition temperature[2,3], ultra-high critical magnetic field[4–6] and potential applications as a group of high T_C superconductors[7,8]. FeSe, with the simplest structure and less toxicity in iron-based superconductors (among all five families), has become one of attractive materials but the T_C is relatively low in bulk state (~8 K)[9]. In the meanwhile, heterostructure based interface engineering has been proved an effective method for raising T_C due to the enhancement of electron-phonon coupling[10] or epitaxial strain[11]. In previous work, *in situ* scanning tunneling microscopy/spectroscopy (STM/STS)[12] and angle resolved photoemission spectroscopy (ARPES)[13–15] detections on 1-UC thick FeSe films on Nb-doped STO (conductive STO) substrates revealed a superconducting energy gap as large as 20 meV and above 15 meV (closing at a temperature of 65 ± 5 K) respectively, indicating a possible T_C higher than 60 K. Following, the T_C above 40 K in 1-UC FeSe films on insulating STO has been demonstrated by direct transport measurements and Meissner effect[7]. However, direct evidence of T_C above 60 K for FeSe films on conductive substrates and systematic transport studies of FeSe films on insulating substrates are still absent.

Experimental

Previous STM/STS study shows square-like 1 × 1 structure with the in-plane lattice constants a = b = 3.82 Å and 20 meV superconducting-like gap for the 1-UC FeSe films on STO substrates[7]. However, by STS detection, semiconducting behavior is observed for the second UC of the FeSe film on STO. Thus, carefully comparison of the transport properties of high quality 1-UC and 2-UC FeSe films on STO substrates becomes necessary. In this paper, we mainly report the electronic transport and diamagnetic results from five typical FeSe films grown by molecular beam epitaxy (MBE) system. Sample No.1 is 1-UC FeSe on conductive STO substrate, samples No.2 and No.3 are 1-UC FeSe films on insulating STO substrates, while samples No.4 and No.5 are 2-UC FeSe films on insulating STO substrates. The 10-UC FeTe protection layers are deposited before the *ex situ* measurements of the films[12]. All FeSe films are 1.5 mm wide and 8 mm long. The distance between the voltage electrodes for the measurement is 1.8 mm for sample No.2, 2.25 mm for sample No.3, 2.0 mm for sample No.4 and 2.75 mm for sample No.5. As for sample No.1, the diamagnetic measurement exhibits that the onset of magnetization drop starts around 85 K, indicating a possible superconductivity up to this high temperature. For samples No. 2–5, thermally activated flux flow (TAFF) behavior and Hall effect are carefully studied. It is found that single-vortex pinning dominates vortex dynamics in low magnetic field region, whereas collective creep becomes important at higher magnetic fields. More interestingly, sign reversal behavior of Hall coefficient (R_H) with temperature is observed.

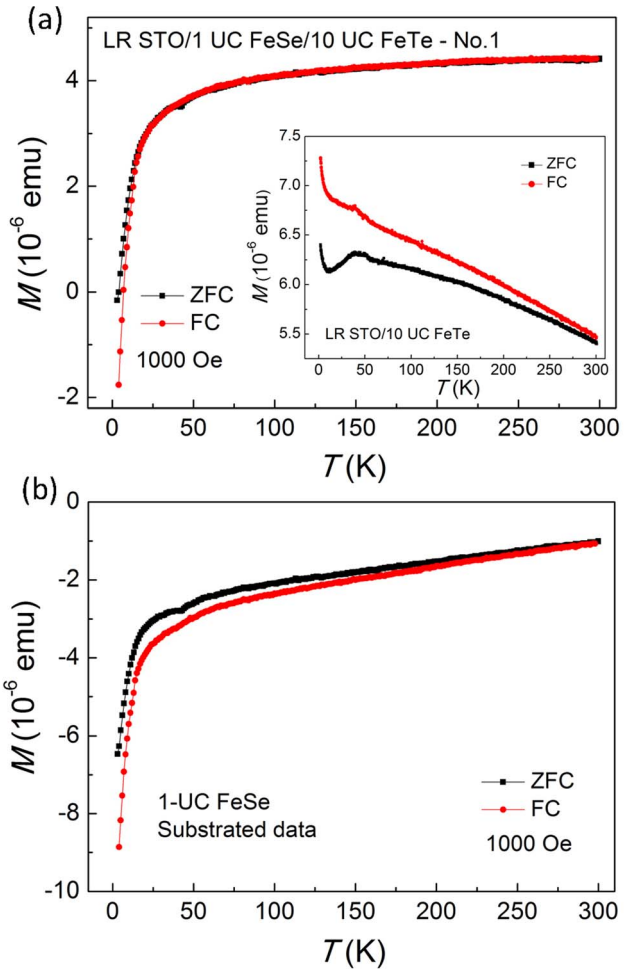

Figure 1 | Diamagnetic measurements of 1-UC FeSe films grown on conductive STO (LR STO) substrate (sample No.1). The *M-T* curves without or with removing the influence of substrate and protection layer show a drop crossover around 85 K. (a) *M-T* curves of sample No.1 (LR STO/1-UC FeSe/10-FeTe) measured under a 1000 Oe parallel magnetic field. Inset: *M-T* curves of LR STO/non-superconducting 1-UC FeSe/10-UC FeTe. (b) *M-T* curves of 1-UC FeSe (removing the influence of STO substrate and FeTe protection layers).

Results and discussions

It is worthy to mention that the observed T_C of 1-UC FeSe on insulating substrate by *ex situ* transport measurements is obvious lower than estimated T_C of 1-UC FeSe on conductive substrate by STM and ARPES studies[12–15]. Indeed, high quality FeSe films are easier to be achieved by MBE growth on conductive STO substrates comparing to insulating STO substrates since the conductive STO substrate shows more flat and homogeneous surface for sample growth. In order to see if higher T_C of 1-UC FeSe can be revealed by direct measurements other than energy gap detection, we did magnetization experiments for 1-UC FeSe on conductive STO substrate (sample No.1) in a magnetic property measurement system (MPMS-SQUID-VSM). DC magnetization as a function of temperature (*M-T*) during both zero field cooling (ZFC) and field cooling (FC) at 1000 Oe parallel field of sample No.1 is shown in Fig. 1(a). The *M-T* curves exhibit a drop crossover around ~85 K. Please notice that the raw data shown in Fig. 1(a) include the contributions from FeSe film, protection layer and STO substrate. Thus, the background signal from the protection layer and substrate is necessary to be subtracted for more precise result. However, it is hard to keep the quality of STO substrates exactly same for magnetic measurements. Therefore, we designed an experiment to exclude the background signal. After we found the 85 K drop crossover of 1-UC FeSe, we put the sample in low vacuum system and waited for a long time until the sample lost its superconductivity. Then, we measured this sample again as the background signal as shown in the inset of Fig. 1(a). We can see that when the sample becomes non-superconducting, the magnetization drop around 85 K disappears. Thus, the possibility of the relation between the drop and the superconductivity cannot be excluded. However, without resistivity evidence of T_C at 85 K, the susceptibility drop alone cannot demonstrate the high T_C up to 85 K in 1-UC FeSe films. Since the susceptibility of FeTe capping layer may also change in the degraded sample, the magnetization curves excluding the background signal shows negative value even at 300 K (Fig. 1b). Interestingly, after subtracting the influence of STO substrate and FeTe protection layer from the same sample, the *M-T* curves still exhibit the magnetization drop crossover around 85 K with decreasing temperature (Fig. 1(b)). The structural phase transition (from a tetragonal to an orthorhombic phase on cooling) of bulk FeSe was ever observed around 90 K[16,17], at which there also is strong antiferromagnetic spin fluctuation[18]. In the meanwhile, phonon softening is a general feature in Fe-based superconductors and induced by either structural phase transition or the superconductive phase transition[18]. Thus, the consideration for the phonon softening may be valuable for understanding our observation of magnetization drop crossover around 85 K in the 1-UC FeSe films, which show much enhanced superconductivity comparing with bulk FeSe.

The electronic transport measurements were carried out in a physical property measurement system with the magnetic field up to 16 T (PPMS-16T). The obtained superconducting parameters of the four measured samples are summarized in Table 1. Figure 2 shows the transport results of sample No.2, one typical 1-UC FeSe film grown on insulating STO substrate covered by non-superconducting FeTe protection layers with an excitation current of 500 nA. Fig. 2(a) shows the sheet resistance of the sample as a function of temperature $R_{sq}(T)$ at zero magnetic field ($\mu_0 H$). The resistance begins to drop at about 54.5 K. By extrapolating both the normal resistance and the superconducting transition curves, we obtain the onset T_c^{onset} = 40.2 K and the resistance drops completely to zero at 23.5 K (T_c^{zero}). The zero resistance is defined when the measured voltage is within the instrumental resolution ± 20 nV. Figure 2(b) shows $R_{sq}(T)$curves at different perpendicular magnetic fields ($\mu_0 H$) up to

Table 1 | Summary of the parameters of four FeSe samples on insulating STO. $T_c^{onset}$was obtained by extrapolating both the normal resistance and the superconducting transition curves. $T_c^{onset}$with star is the temperature at which the resistance starts to decrease. Since previous STM study[11] indicates that the second UC of FeSe films grown on STO substrates shows semiconducting behavior and only the first UC FeSe is superconducting, J_C of the four samples at 2 K is calculated from I_C by using the thickness of 0.55 nm (1-UC FeSe)

T_C^{onset} (K)				T_C^{zero} (K)				J_C (A/cm^2)			
1-UC (No.2)	1-UC (No.3)	2-UC (No.4)	2-UC (No.5)	1-UC (No.2)	1-UC (No.3)	2-UC (No.4)	2-UC (No.5)	1-UC (No.2)	1-UC (No.3)	2-UC (No.4)	2-UC (No.5)
40.2 K *54.5 K	36.0 K *45.8 K	43.0 K *50.0 K	40.0 K *55.0 K	23.5 K	2.3 K	22.5 K	16.5 K	1.67×10^6	4.85×10^4	2.72×10^5	9.7×10^5

16 T from 2 K to 60 K. The resistive transition becomes broader and shifts to lower temperatures with increasing magnetic field, characteristic of superconducting transition in thin films.

We know in the thermally activated flux flow (TAFF) of vortex region, the $\ln\rho - 1/T$ can be described by Arrhenius relation[19,20]

$$\rho(T,H) = \rho_0(H)\, exp[-U_0(H)/T] \quad (1)$$

where ρ_0 is a temperature independent constant and $U_0(H)$ is the activation energy of the flux flow. Thus, $\ln\rho(T,H)$ versus $1/T$ should be linear in the TAFF region. As shown in Fig. 2(c), the experimental data in Fig. 2(b) can be well fitted by the Arrhenius relation (solid lines). The fitting lines obtained from $\ln\rho(T,H)$ versus $1/T$ at different magnetic fields can be well extrapolated to the same temperature, T_m = 38 K, which is close to the value of T_c^{onset}. In addition, the activation energy U_0 for different magnetic field can be obtained by the slope of the solid fitting lines. As shown in Fig. 2(d), the $U_0(H)$ shows a magnetic field dependent power law relation,

$$U_0(H) \propto H^{-\alpha} \quad (2)$$

with α = 0.14 ($\mu_0 H < 3.4$ T) and 0.60 ($\mu_0 H > 3.4$ T), respectively.

For the 2-UC FeSe film grown on insulating STO substrate covered by non-superconducting FeTe protection layer (sample No.4), Fig. 3(a) shows the sheet resistance as a function of temperature $R_{sq}(T)$ at zero magnetic field ($\mu_0 H$). By extrapolating both the normal resistance and the superconducting transition curves, we obtain the onset T_c^{onset} = 43 K and the resistance drops completely to zero at 22.5 K (T_c^{zero}), which are almost same with those of 1-UC FeSe (sample No.2). Figure 3(b) shows the R_{sq} of sample No.4 as a function of temperature, $R_{sq}(T)$, at different perpendicular magnetic fields ($\mu_0 H$). The $R_{sq}(T)$ curves at different magnetic fields can also be fitted by the Arrhenius relation (solid lines) well as shown in Fig. 3(c). The fitting lines obtained from $\ln\rho(T,H)$ versus $1/T$ at different magnetic fields cross to one point at about T_m = 36 K, which is consistent with the T_C of the sample. The activation energy U_0 varies with different magnetic field can be achieved by the slope of the solid fitting lines as shown in Fig. 3(d), α = 0.125 ($\mu_0 H < 3.7$ T) and 0.79 ($\mu_0 H > 3.7$ T) respectively by utilizing Eq. (2). These values obtained from the two samples are close. At the temperatures not far from T_C, the weak power law decreases of $U_0(H)$ in low magnetic fields for both samples implies that single-vortex pinning dominates in this region, followed by a quicker decrease of $U_0(H)$ at high field where a crossover to collective flux creep regime occurs. The similar behaviors are observed in iron-based superconductors, such as FeSe[21,22], FeTeSe[23] and Nd(O,F)FeAs[24] crystals. The exponent α = 0.5 and 1 corresponds to a planar-defect pinning and a point-defect pinning in high T_C superconductors respectively[25]. For our FeSe ultrathin films, the fitted values obtained at high magnetic field vary between 0.5 and 1, suggesting that the pinning centers may be mixed with point and planar defects. The cross-over magnetic field is about 3 T for bulk FeSe, 2 T for FeTeSe, and 3 T for Nd(O,F)FeAs, which are almost in the same level with our observation in ultrathin FeSe films. For cuprates, the range of the cross-over magnetic field is from 0.8 T - 5.5 T, where the exact value depends on the sample situations, such as defects and boundaries.

The Hall resistance (R_{xy}) of FeSe films is measured by sweeping the magnetic field at a fixed temperature. The temperature stabilization is better than 0.1%. The distance between the Hall voltage electrodes is about 1.5 mm for all measured samples. Figures 4(a)–4(b) show the data of R_{xy} vs magnetic field ($R_{xy}(H)$) at different temperatures from 40 K to 150 K of samples No.2 and No.4, which exhibit good linear relation. In order to subtract the influence of FeTe protection layer, transport properties of reference sample (10 UC FeTe grown on insulating STO substrate) were studied. The sheet resistance of the reference sample varies with temperature ($R_{sq}(T)$) under different magnetic fields (0 T, 9 T and −9 T) are exhibited in Fig. 4(c). Figure 4(d) shows the $R_{xy}(H)$ curves of the reference sample at

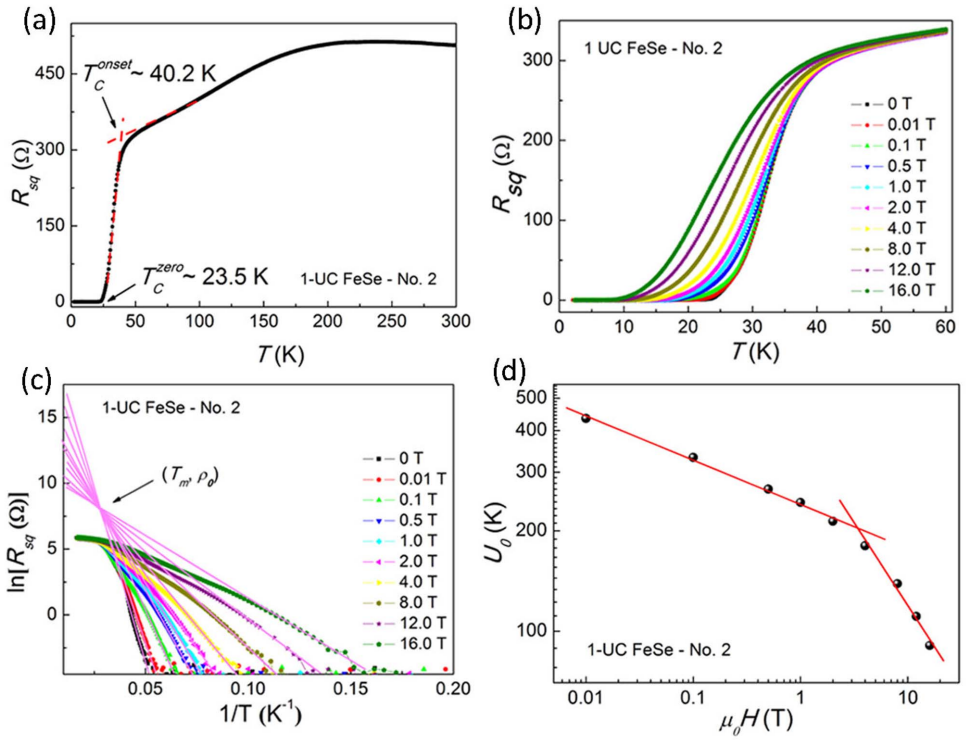

Figure 2 | Transport measurement of the 1-UC FeSe film grown on insulating STO (HR STO) substrate (sample No.2). (a) The temperature dependence of sheet resistance under zero field, showing T_c^{onset} = 40.2 K and T_c^{zero} = 23.5 K. (b) The temperature dependence of sheet resistance under various perpendicular magnetic fields up to 16 T, showing a typical broadened superconducting transition. (c) $ln[R_{sq}(\Omega)]$ *vs.* $1/T$ in various perpendicular magnetic fields. The corresponding solid lines are fitting results from the Arrhenius relation. (d) Field dependence of $U_0(H)$. The solid lines are power-law fits using $U_0(H) \sim H^{-\alpha}$. For this 1-UC FeSe film, α = 0.14 for $\mu_0 H < 3.4$ T, and α = 0.60 for $\mu_0 H > 3.4$ T.

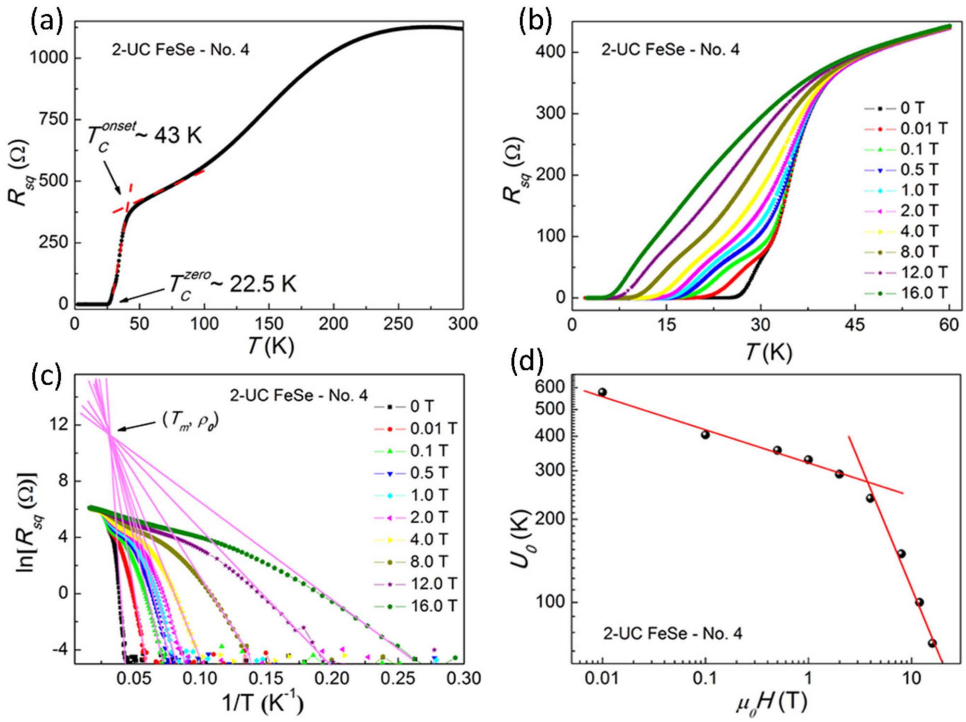

Figure 3 | Transport measurement of the 2-UC FeSe film grown on HR STO substrate (sample No.4). (a) The temperature dependence of sheet resistance under zero field, showing $T_c^{onset} = 43K$ and $T_c^{zero} = 22.5K$. (b) The temperature dependence of sheet resistance under various perpendicular magnetic fields. (c) $ln[R_{sq}(\Omega)]$ *vs.* $1/T$ in various perpendicular magnetic fields. The corresponding solid lines are fitting results from the Arrhenius relation. (d) Field dependence of $U_0(H)$. The solid lines are power-law fits using $U_0(H) \sim H^{-\alpha}$. For this 2-UC FeSe film, $\alpha = 0.125$ for $\mu_0 H < 3.7$ T, and $\alpha = 0.79$ for $\mu_0 H > 3.7$ T.

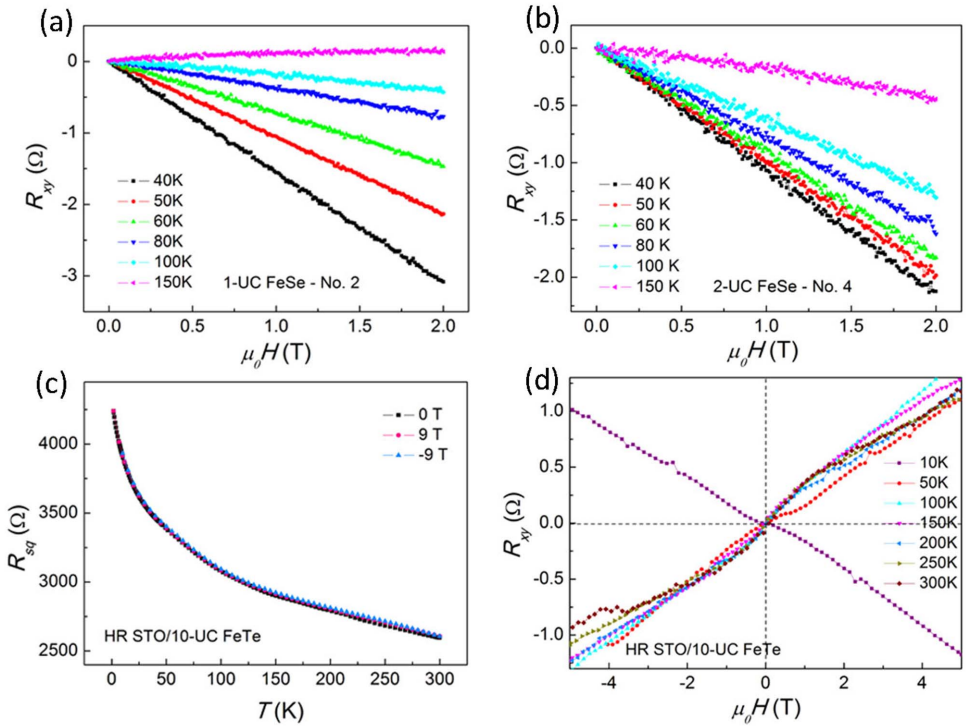

Figure 4 | Hall results of FeSe films and FeTe protection layers. (a) Hall resistance (R_{xy}) varies with magnetic field — $R_{xy}(H)$ at different temperatures of sample No.2. (b) $R_{xy}(H)$ curves at different temperatures of sample No.4. (c) $R_{sq}(T)$ curves of the 10-UC FeTe protection layer under different perpendicular magnetic fields (0 T, 9 T and −9 T). (d) $R_{xy}(H)$ curves at different temperatures of the 10-UC FeTe protection layer.

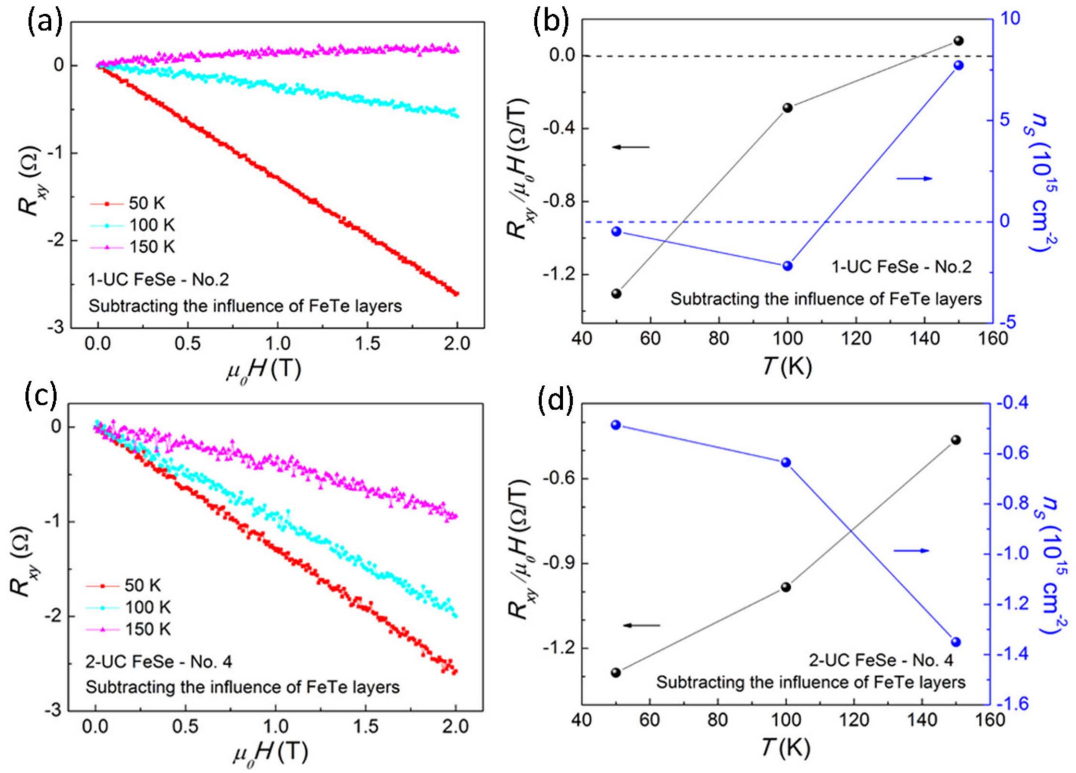

Figure 5 | Hall results of sample No.2 (1-UC FeSe films grown on HR STO) and sample No.4 (2-UC FeSe films grown on HR STO) after subtracting the influence of the protection layer. (a) & (c), R_{xy} vs magnetic field curves at different temperatures of sample No.2 and No.4 subtracting the background of protection layers, respectively. (b) & (d), Hall sensitivity and the carrier density of sample No.2 and No.4 at different temperatures obtained from the data in (a) and (c).

different temperatures. The Hall conductance of pure FeSe films (removed the influence of FeTe layers) can be calculated by $\sigma_{xy(FeSe)} = \sigma_{xy(sample)} - \sigma_{xy(FeTe)}$ ($\sigma_{xy} = -\frac{R_{sq(xy)}}{R^2_{sq(xx)} + R^2_{sq(xy)}}$). After removing the influence of FeTe protection layer, the Hall resistance ($R_{sq(xy)\text{-}FeSe}$) of the pure FeSe film sample is re-obtained by conversing from Hall conductance of FeSe films, $R_{sq(xy)-FeSe} = -\frac{\sigma_{xy(FeSe)}}{\sigma^2_{xx(FeSe)} + \sigma^2_{xy(FeSe)}}$ (where $\sigma_{xx} = \frac{R_{sq(xx)}}{R^2_{sq(xx)} + R^2_{sq(xy)}}$), which are plotted in Figs. 5(a) and 5(c) for sample No.2 and No.4, respectively.

In Fig. 5(b), the temperature dependence of the Hall sensitivity $\frac{R_H}{d} = \frac{V_H}{I(\mu_0 H)} = \frac{R_{xy}}{\mu_0 H}$ (V_H is the Hall voltage, d is the thickness of the sample) and two-dimensional carrier density ($n_s = \frac{1}{(R_H/d)\cdot q} = \frac{1}{(R_{xy}/\mu_0 B)\cdot q}$, q is the charge of electron) are plotted. For a normal metal with Fermi liquid feature, the Hall coefficient is constant at different temperatures. However, it varies with temperature for multiband materials, such as MgB_2[26], iron-based superconductors[27], or a sample with non-Fermi liquid behavior such as cuprate superconductors[28]. Here, an interesting phenomenon—sign reversal behavior of $\frac{R_H}{d}$ is observed in the 1-UC FeSe film (sample No.2) with temperature increasing (shown in Fig. 5(a) and 5(b)). In Fig. 5(a), the slope of the $R_{xy}(H)$ curves changes from negative to positive as the temperature is higher than 100 K. Correspondingly, the signs of $\frac{R_H}{d}$ and n_s reversed at the same time as shown in Fig. 5(b). That is to say, as the temperature is lower than 100 K, the 1-UC FeSe film is electron-doped, but it is hole-doped while the temperature higher than 100 K. As for 2-UC FeSe film, Figure 5(c) shows the $R_{xy}(H)$ curves of sample No.4 at different temperatures from 40 K to 150 K. The Hall sensitivity $\frac{R_H}{d}$ for sample No.4 decays continuously with increasing temperature as shown in Fig. 5(d). The value of $\frac{R_H}{d}$ at 150 K is almost 10 times smaller than that at 40 K, exhibiting strong temperature dependence of $\frac{R_H}{d}$. This behavior is possibly induced by the multiband effect. For sample No.4, the Hall data manifest electron-doped property as increasing temperature till 150 K. Please notice that the carrier density (n_s) in FeSe films is pretty huge ($\sim 10^{15}$ cm^{-2}).

In order to confirm that the sign reversal of $\frac{R_H}{d}$ is a universal behavior in ultrathin FeSe films, Hall resistance from another two samples (sample No.3 is 1-UC FeSe film and sample No.5 is 2-UC FeSe film) at various temperatures up to 300 K was measured. Figure 6(a) and 6(b) are the raw $R_{xy}(H)$ data from sample No.3 and No.5. The signs of $\frac{R_H}{d}$ are obviously reversed in these two samples with increasing temperature. After subtracting the influence of FeTe protection layer utilizing the same method mentioned above, the R_{xy} curves of pure FeSe films at different temperatures are shown in Fig. 6(c)–6(f) with similar sign reversal behavior of $\frac{R_H}{d}$. The parameters of Hall effect for all four samples can be found in Table 2 & 3. Thus, the crossover of conduction carrier type with temperature is demonstrated to be a universal phenomenon for ultrathin FeSe films. The reversal temperature is 80 K or 150 K for 1-UC FeSe films (sample No.3 or sample No.2) but 150 K or larger for 2-UC FeSe (sample No.5 or sample No.4).

Interestingly, we found that the sign reversal behavior of the Hall results of our FeSe films always happens at the temperature before

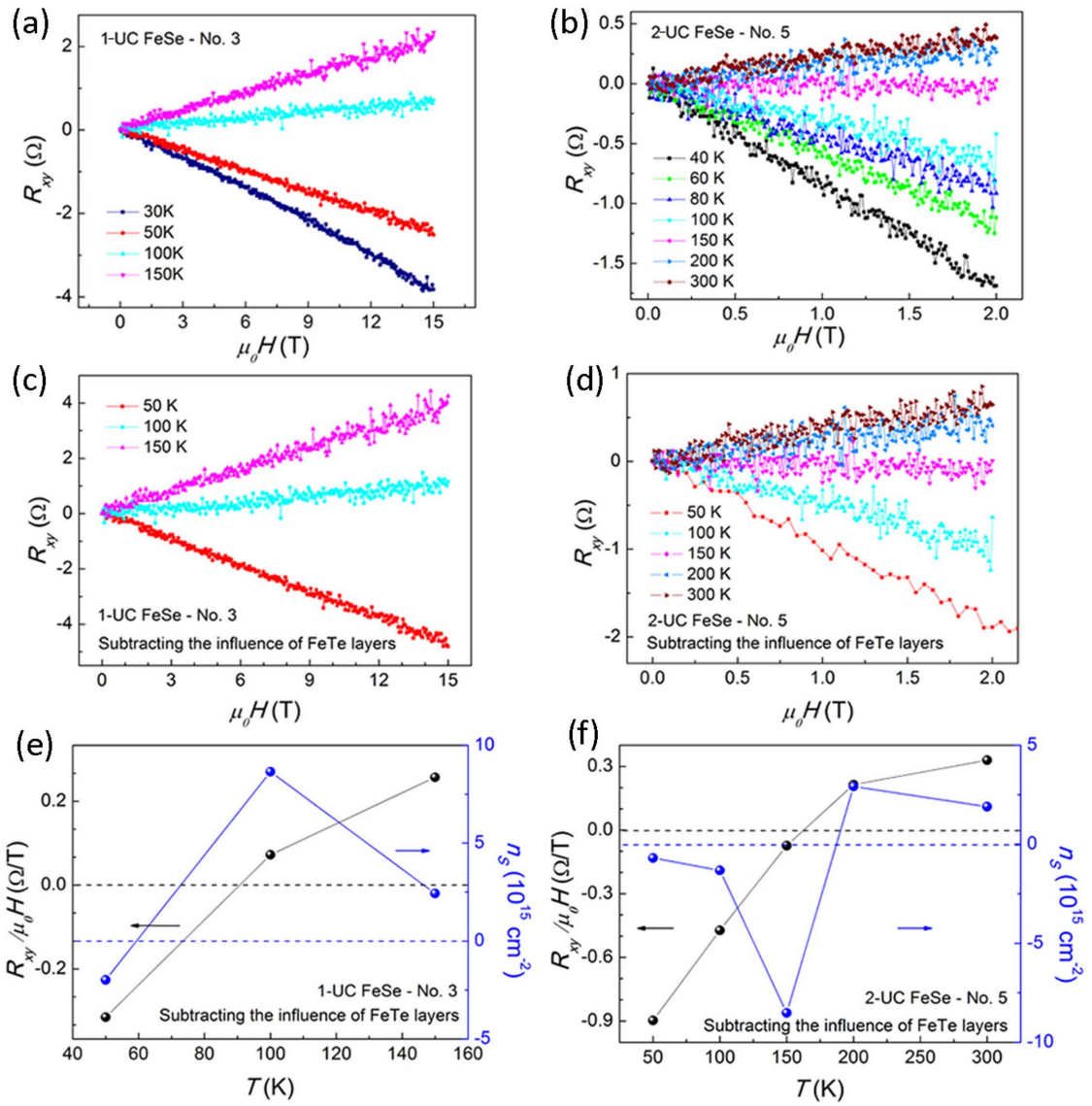

Figure 6 | Hall results of sample No.3 (1-UC FeSe films grown on HR STO) and sample No.5 (2-UC FeSe films grown on HR STO). (a) $R_{xy}(H)$ curves at different temperatures of sample No.3. (b) $R_{xy}(H)$ curves at different temperatures of sample No.5. (c) & (d) $R_{xy}(H)$ curves at different temperatures of sample No.3 and No.5 subtracting the background, respectively. (e) & (f) Hall coefficient and the carrier density of sample No.3 and No.5 at different temperatures after subtracting the background.

Table 2 | Hall sensitivity carrier density and mobility of four FeSe samples on HR STO at different temperatures (with FeTe protection layer)

T (K)	$R_{xy}/\mu_0 B$ (Ω/T)				n_S (10^{15} cm^{-2})				Mobility (cm^2/Vs)			
	1-UC (No.2)	1-UC (No.3)	2-UC (No.4)	2-UC (No.5)	1-UC (No.2)	1-UC (No.3)	2-UC (No.4)	2-UC (No.5)	1-UC (No.2)	1-UC (No.3)	2-UC (No.4)	2-UC (No.5)
30 K		−0.221				−2.828				2.290		
40 K	−1.545	−0.220	−1.073	−0.845	−0.405	−2.836	−0.583	−0.740	52.150	1.971	30.970	12.382
50 K	−1.069	−0.164	−0.990	−0.322	−0.585	−3.811	−0.632	−0.937	32.354	1.435	24.110	8.935
60 K	−0.732	−0.104	−0.917	−0.589	−0.854	−6.013	−0.681	−1.060	23.446	0.903	20.752	7.623
80 K	−0.390	−0.017	−0.790	−0.440	−1.6	−35.837	−0.791	−1.422	11.628	0.150	15.931	5.40
100 K	−0.212	0.062	−0.643	−0.335	−2.96	10.158	−0.973	−1.865	5.859	0.523	11.437	3.900
150 K	0.086	0.174	−0.220	−0.017	7.29	3.601	−2.84	−35.755	2.022	1.423	2.746	0.173
200 K		0.214		0.137		2.921		4.552		1.737		1.223
300 K		0.188		0.197		3.320		3.172		1.583		1.720

Table 3 | Hall sensitivity carrier density and mobility of four samples on HR STO subtracting the influence of FeTe protection layer at different temperatures (subtracting FeTe affection)

T (K)	$R_{xy}/\mu_0 B$ (Ω/T)				n_S (10^{15} cm^{-2})				Mobility (cm^2/Vs)			
	1-UC (No.2)	1-UC (No.3)	2-UC (No.4)	2-UC (No.5)	1-UC (No.2)	1-UC (No.3)	2-UC (No.4)	2-UC (No.5)	1-UC (No.2)	1-UC (No.3)	2-UC (No.4)	2-UC (No.5)
50 K	−1.305	−0.315	−1.287	−0.897	−0.179	−1.985	−0.486	−0.697	39.516	3.719	31.343	19.827
100 K	−0.286	0.072	−0.984	−0.473	−2.183	8.648	−0.635	−1.322	7.138	0.830	17.516	9.072
150 K	0.081	0.257	−0.463	−0.073	7.719	2.432	−1.350	−8.522	1.719	2.432	5.776	1.197
200 K				0.214				2.917				3.149
300 K				0.329				1.897				4.744

the hump of the $R_{sq}(T)$ curves, thus, a possible structural transition of FeSe film may contribute to the observed sign reversal phenomenon[16,17,29]. Besides, we notice that similar sign reversal behavior was also observed in topological insulator Bi_2Te_3[30] and was attributed to the change of defects in the sample. Further experimental or theoretical investigations in this context would be valuable towards the comprehension of the observed sign reversal Hall effect in 1-UC FeSe films.

The origins of the huge interface-induced enhancement of T_C in 1-UC FeSe films compared with bulk FeSe are still under debate and many possible factors may contribute. An early magnetic study on the single-crystalline $Fe_{1.02}Se$ reveals that T_C can be increased from 7 K to above 30 K with the modest pressure range below 2 GPa[31]. Additionally, doubling the critical temperature of $La_{1.9}Sr_{0.1}CuO_4$ using epitaxial strain was also reported[11]. However, for 1-UC FeSe films on STO, the in-plane lattice constant measured from the atomically resolved STM image is ~3.82 Å[7], which is a little larger than the bulk value (3.77 Å) while still smaller than the in-plane lattice constant of STO (001) surface (3.91 Å), indicating that the tensile train in the 1-UC FeSe films is less than 1%. Furthermore, FeSe and Fe(Se,Te) films grown on different substrates with larger lattice constants, such as MgO, Si, and Al_2O_3, were studied[32]. The observed T_C of these films is not higher than 20 K although the tensile strain in these films is much larger than our situation. Therefore, we conclude that the small tensile strain alone in 1-UC FeSe films cannot explain the observed high T_C superconductivity. As has been revealed by recent *in situ* ARPES study[15] and calculation[33,34], the charge transfer from the oxygen vacancy states of the STO substrate may play an important role in the high T_C superconductivity[33]. Additionally, the soft phonons at the interface can enhance the energy scale of Cooper pairing and even change the pairing symmetry, then may increase the T_C[34,35].

In summary, superconducting properties of ultra-thin (1-UC or 2-UC) FeSe films grown on insulating STO and conductive STO substrates were studied by transport and magnetic measurements. *M-T* observation of FeSe films on conductive STO shows a susceptibility drop ~85 K. Further transport investigations are necessary to see if the drop is corresponding to the superconductivity. The results from films on insulating STO reveal Arrhenius TAFF behavior with a transition from single-vortex pinning region to collective creep region. More intriguingly, the observed sign reversal of Hall coefficient above T_C demonstrates a crossover from hole transport to electron conduction in ultrathin FeSe films with decreasing temperature.

1. Kamihara, Y., Watanabe, T., Hirano, M. & Hosono, H. Iron-Based Layered Superconductor $La[O_{1-x}F_x]FeAs$ (x = 0.05–0.12) with T_C = 26 K. *J. Am. Chem. Soc.* **130**, 3296–3297 (2008).
2. Ren, Z. *et al.* Superconductivity at 55 K in Iron-Based F-Doped Layered Quaternary Compound $Sm[O_{1-x}F_x]FeAs$. *Chin. Phys. Lett.* **25**, 2215–2216 (2008).
3. Wang, C. *et al.* Thorium-doping–induced superconductivity up to 56 K in $Gd_{1-x}Th_xFeAsO$. *Euro. Phys. Lett.* **83**, 67006 (2008).
4. Mizuguchi, Y. *et al.* Superconductivity at 27 K in tetragonal FeSe under high pressure. *Appl. Phys. Lett.* **93**, 152505 (2008).
5. Hunte, F. *et al.* Two- band superconducticity in $LaFeAsO_{0.89}F_{0.11}$ at very high magnetic fields. *Nature* **453**, 903 (2008).
6. Yuan, H. Q. *et al.* Nearly isotropic superconductivity in (Ba, K)Fe_2As_2. *Nature* **457**, 565 (2009).
7. Zhang, W. H. *et al.* Direct Observation of High-Temperature Superconductivity in One-Unit-Cell FeSe Films. *Chin. Phys. Lett.* **31**, 017401 (2014).
8. Lei, H. C., Hu, R. W. & Petrovic, C. Critical fields, thermally activated transport, and critical current density of β-FeSe single crystals. *Phys. Rev. B* **84**, 014520 (2011).
9. Hsu, F. C. *et al.* Superconductivity in the PbO-type structure α-FeSe. *Proc. Natl. Acad. Sci. USA* **105**, 14262 (2008).
10. Strongin, M. *et al.* Enhanced superconductivity in layered metallic films. *Phys. Rev. Lett.* **21**, 1320–1323 (1968).
11. Locquet, J. P. *et al.* Doubling the critical temperature of $La_{1.9}Sr_{0.1}CuO_4$ using epitaxial strain. *Nature* **394**, 453 (1998).
12. Wang, Q. Y. *et al.* Interface-induced high-temperature superconductivity in single unit-cell FeSe films on $SrTiO_3$. *Chin. Phys. Lett.* **29**, 037402 (2012).
13. Liu, D. *et al.* Electronic origin of high-temperature superconductivity in single-layer FeSe superconductor. *Nature Commun.* **3**, 931 (2012).
14. He, S. *et al.* Phase diagram and high temperature superconductivity at 65 K in tuning carrier concentration of single-layer FeSe films. *Nat. Mater.* **12**, 605 (2013).
15. Tan, S.-Y. *et al.* Interface-induced superconductivity and strain-dependent spin density wave in FeSe/$SrTiO_3$ thin films. *Nat. Mater.* **12**, 634 (2013).
16. Margadonna, S. *et al.* Crystal structure of the new $FeSe_{1-x}$ superconductor. *Chem. Commun.* **43**, 5607 (2008).
17. McQueen, T. M. *et al.* Tetragonal-to-Orthorhombic Structural Phase Transition at 90 K in the Superconductor $Fe_{1.01}Se$. *Phys. Rev. Lett.* **103**, 057002 (2009).
18. Luo, C. W. *et al.* Quasiparticle Dynamics and Phonon Softening in FeSe Superconductors. *Phys. Rev. Lett.* **108**, 257006 (2012).
19. Palstra, T. T. M., Batlogg, B., Schneemeyer, L. F. & Waszczak, J. V. Thermally Activated Dissipation in $Bi_{2.2}Sr_2Ca_{0.8}Cu_2O_{8+\delta}$. *Phys. Rev. Lett.* **61**, 1662 (1988).
20. Palstra, T. T. M., Batlogg, B., van Dover, R. B., Schneemeyer, L. F. & Waszczak, J. V. Dissipative flux motion in high-temperature superconductors. *Phys. Rev. B* **41**, 6621 (1990).
21. Lei, H. C., Hu, R. W. and Petrovic, C. Critical fields, thermally activated transport, and critical current density of *β*-FeSe single crystals. *Phys. Rev. B* **84**, 014520 (2011).
22. Lei, H. C. *et al.* Iron chalcogenide superconductors at high magnetic fields. *Sci. Technol. Adv. Mater.* **13**, 054305 (2012).
23. Ge, J. Y. *et al.* Superconducting properties of highly oriented $Fe_{1.03}Te_{0.55}Se_{0.45}$ with excess Fe. *Solid State Communications* **150**, 1641 (2010).
24. Jaroszynski, J. *et al.* Upper critical fields and thermally-activated transport of $NdFeAsO_{0.7}F_{0.3}$ single crystal. *Phys. Rev. B* **78**, 174523 (2008).
25. Chin, C. C. & Morishita, T. The transport properties of $YBa_2Cu_3O_{7-x}$ thin films. *Physica C* **207**, 37–43 (1993).
26. Yang, H. *et al.* Fully Band-resolved scattering rate in MgB_2 revealed by the nonlinear Hall effect and magnetoresistance measurements. *Phys. Rev. Lett.* **101**, 067001 (2008).
27. Cheng, P. *et al.* Hall effect and magnetoresistance in single crystals of $NdFeAsO_{1-x}F_x$ (x = 0 and 0.18). *Phys. Rev. B* **78**, 134508 (2008).
28. Ong, N. P. The Hall Effect and its Relation to other Transport Phenomena in the Normal State of the High-Temperature Superconductor. *Physical Properties of High-Temperature Superconductors.* Ginsberg, D. M. (ed.) 459–507 (World Scientific, Singapore, 1990).
29. Millican, J. N. *et al.* Pressure-induced effects on the structure of the FeSe superconductor. *Solid State Communications* **149**, 707 (2009).
30. Hor, Y. S., Qu, D., Ong, N. P. & Cava, R. J. Low temperature magnetothermoelectric effect and magnetoresistance in Te vapor annealed Bi_2Te_3. *J. Phys.: Condens. Matter* **22**, 375801 (2010).
31. Tissen, V. G. *et al.* Effects of pressure-induced phase transitions on superconductivity in single-crystal $Fe_{1.02}Se$. *Phys. Rev. B* **80**, 092507 (2009).
32. Li, Q. *et al.* Films of iron chalcogenide superconductors. *Rep. Prog. Phys.* **74**, 124510 (2011).

33. Liu, K. Lu, Z. Y. & Xiang, T. Atomic and electronic structures of FeSe monolayer and bilayer thin films on $SrTiO_3$ (001): First-principles study. *Phys. Rev. B* **85**, 235123 (2012).
34. Xiang, Y.-Y., Wang, F., Wang, D., Wang, Q.-H. & Lee, D.-H. High-temperature superconductivity at the FeSe/$SrTiO_3$ interface. *Phys. Rev. B* **86**, 134508 (2012).
35. Lee, J. J. *et al.* Significant Tc enhancement in FeSe films on $SrTiO_3$ due to anomalous interfacial mode coupling. *arXiv:1312.2633v4.*

Acknowledgments

The authors thank Fa Wang, Zhili Xiao, Jiyong Yang and Mingliang Tian for fruitful discussions. This work was financially supported by National Basic Research Program of China (Grant Nos. 2013CB934600 & 2012CB921300), the National Natural Science Foundation of China (Nos. 11222434, 11174007, 91121004, 11321091 and 11374336), the Research Fund for the Doctoral Program of Higher Education (RFDP) of China and China Postdoctoral Science Foundation (No. 2011M500180 & No. 2012T50012).

Author contributions

J.W., L.W., X.M. and Q.-K.X. designed and coordinated the experiments; Y.S., W.Z., Y.X., F.L., Y.Z., Z.X. and J.W. carried out the experiments; Y.S. and J.W. wrote the paper.

Additional information

Competing financial interests: The authors declare no competing financial interests.

How to cite this article: Sun, Y. *et al.* High temperature superconducting FeSe films on $SrTiO_3$ substrates. *Sci. Rep.* **4**, 6040; DOI:10.1038/srep06040 (2014).